Climate Model Downscaling: Spatial Models and Uncertainty Quantification

Emily L. Kang

Division of Statistics and Data Science
Department of Mathematical Sciences
University of Cincinnati

IMSI, May 2025

This research is joint with Ayesha Ekanayaka (University of North Carolina), Peter Kalmus (Jet Propulsion Laboratory, California Institute of Technology), Amy Braverman (Jet Propulsion Laboratory, California Institute of Technology), Hancheng Li (UC), and Alex Konomi (UC).

Outlines

Introduction

- Computer simulations and models are widely used to explore and analyze complex systems.
- One example of such computer models is climate models. They are the primary tools used by scientists to study the climate system and assess its potential impacts.
  - **Global climate models (GCMs)** have been developed to simulate the entire Earth's climate systems.
  - As part of the **Coupled Model Intercomparison Project Phase 6 (CMIP6)**, research teams around the world contribute simulations using their own GCMs.
  - The **CMIP6 ScenarioMIP (Scenario Model Intercomparison Project)** is one of the core CMIP6 experiments. It coordinates climate model simulations to explore potential future climate outcomes under different greenhouse gas emission and land-use scenarios.

Challenges When Using GCM Outputs

- **Computational demands**: Running GCMs and storing GCM outputs requires substantial computational resources and data storage capacity.
- **Model evaluation and comparison**:
  - Different modeling groups make varying assumptions (e.g., cloud formation) and tune model parameters differently, leading to structural differences across models.
- **Model biases**: GCMs often exhibit systematic errors in simulating key climate variables.
  $\rightarrow$ Bias correction is typically required.
- **Coarse spatial resolution** (typically 100–300 km): Limits the ability to capture local and regional patterns that are critical for management and decision-making.
  $\rightarrow$ **Downscaling is needed!**

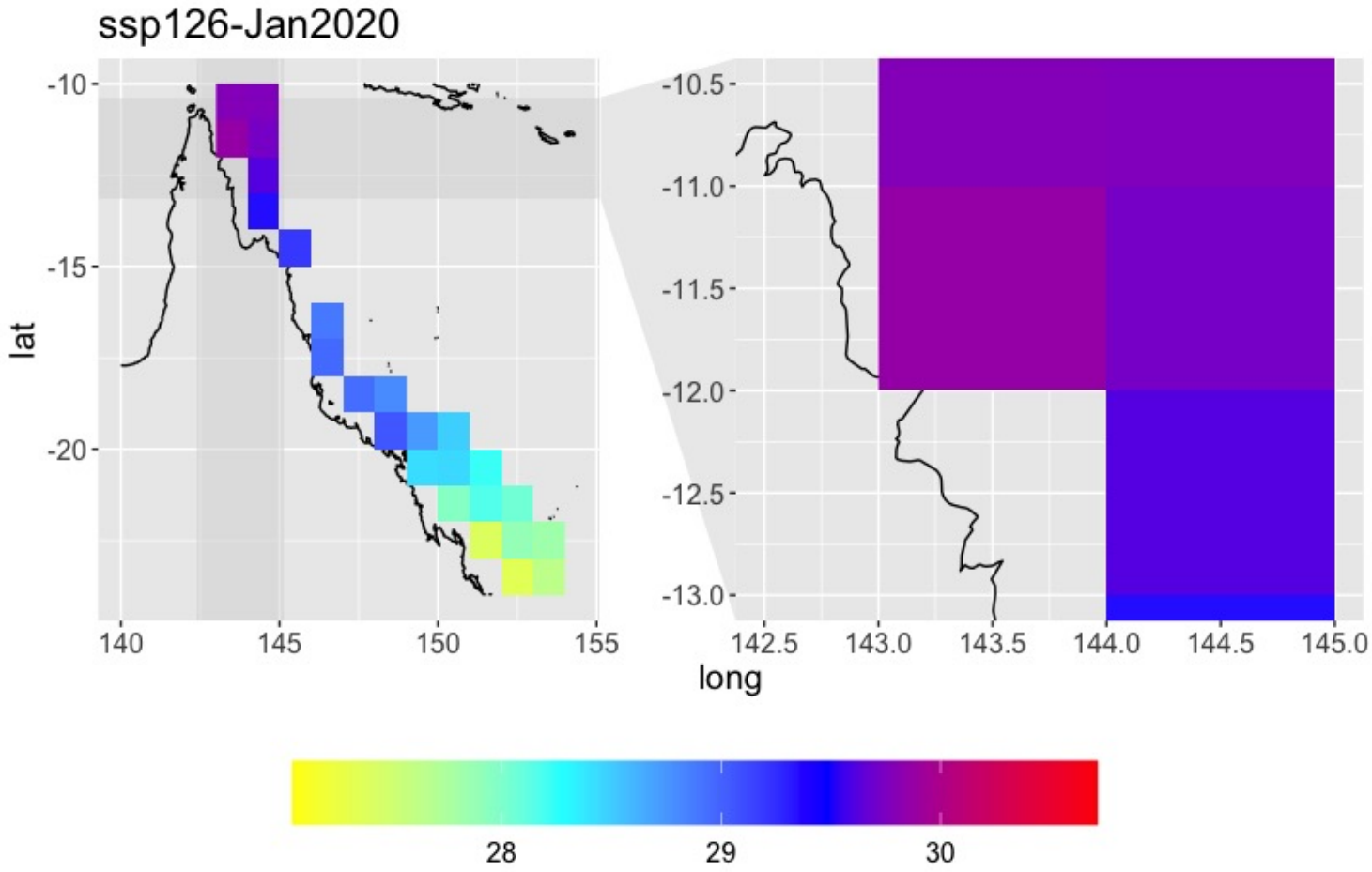
ssp126-Jan2020
lat
-10
-15
-20
140
145
150
155
-10.5
-11.0
-11.5
-12.0
-12.5
-13.0
142.5
143.0
143.5
144.0
144.5
145.0
long
28
29
30

Climate Model Downscaling

- There are two main approaches to downscaling climate model outputs:
  - **Dynamical downscaling**: Uses high-resolution regional climate models (RCMs) driven by boundary conditions from a GCM.
  - **Statistical downscaling**: Develops statistical relationships to translate coarse-resolution GCM outputs into finer-scale climate information.
- Dynamical downscaling is **physics-driven** and typically **computationally intensive**.
- Statistical downscaling is **data-driven** and more **computationally efficient**.
- **Uncertainty quantification (UQ)** of downscaled outputs is essential for reliable downstream analyses and informed decision-making.

Motivation

- Coral reefs, often called the "rainforests of the sea," are vital marine ecosystems. They support immense biodiversity, protect coastlines, and sustain millions of livelihoods worldwide.
- Coral bleaching is triggered by stressful environmental conditions—most commonly high temperatures (Hughes et al., 2003; Hoegh-Guldberg et al., 2007; Gattuso et al., 2015; Masson-Delmotte et al., 2018).
  - *"84% of the world's coral reefs hit by worst bleaching event on record"* — AP News, April 2025

Bleaching is visible on coral reef off the coast of Nha Trang, Vietnam, Oct. 24, 2024. (AP Photo/Yannick Peterhans, File)

Downscaling Sea Surface Temperature (SST)

- The Coral Reef Watch program (Liu et al., 2003, 2006) developed a thermal stress index based on sea surface temperature (SST) data.

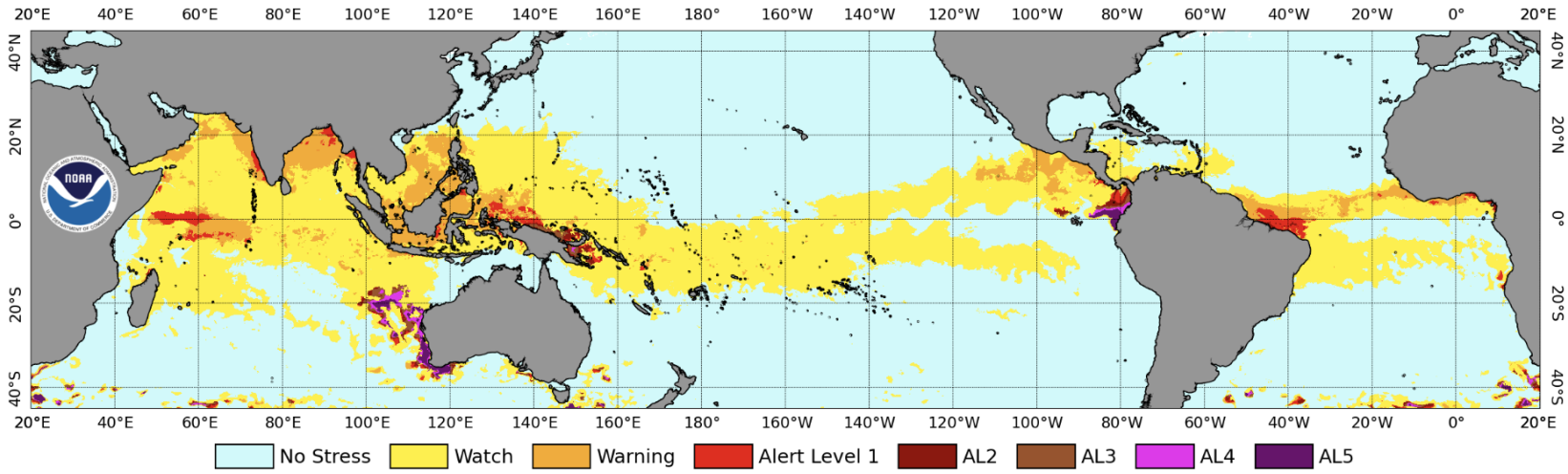

- Downscaled SST is essential for accurately computing such indices, understanding the timing and severity of coral bleaching events, and supporting local conservation and management efforts (Van Hooidonk et al., 2015).

Data

- Our study focuses on the Great Barrier Reef (GBR) region, home to the world's largest coral ecosystem.
- We used monthly NASA/JPL Multiscale Ultrahigh Resolution (MUR) satellite sea surface temperature (SST) data at 1 km resolution, spanning June 2002 to December 2020, covering over 300,000 pixels in the study area.
- Our goal is to downscale monthly SST outputs from a CMIP6 GCM at 100 km resolution to 1 km, leveraging the MUR data product, under two scenarios representing different Shared Socioeconomic Pathways (SSPs) with Representative Concentration Pathways (RCPs):
  - **SSP126**: Low emissions scenario with strong mitigation efforts.
  - **SSP585**: High emissions scenario driven by fossil-fueled development.

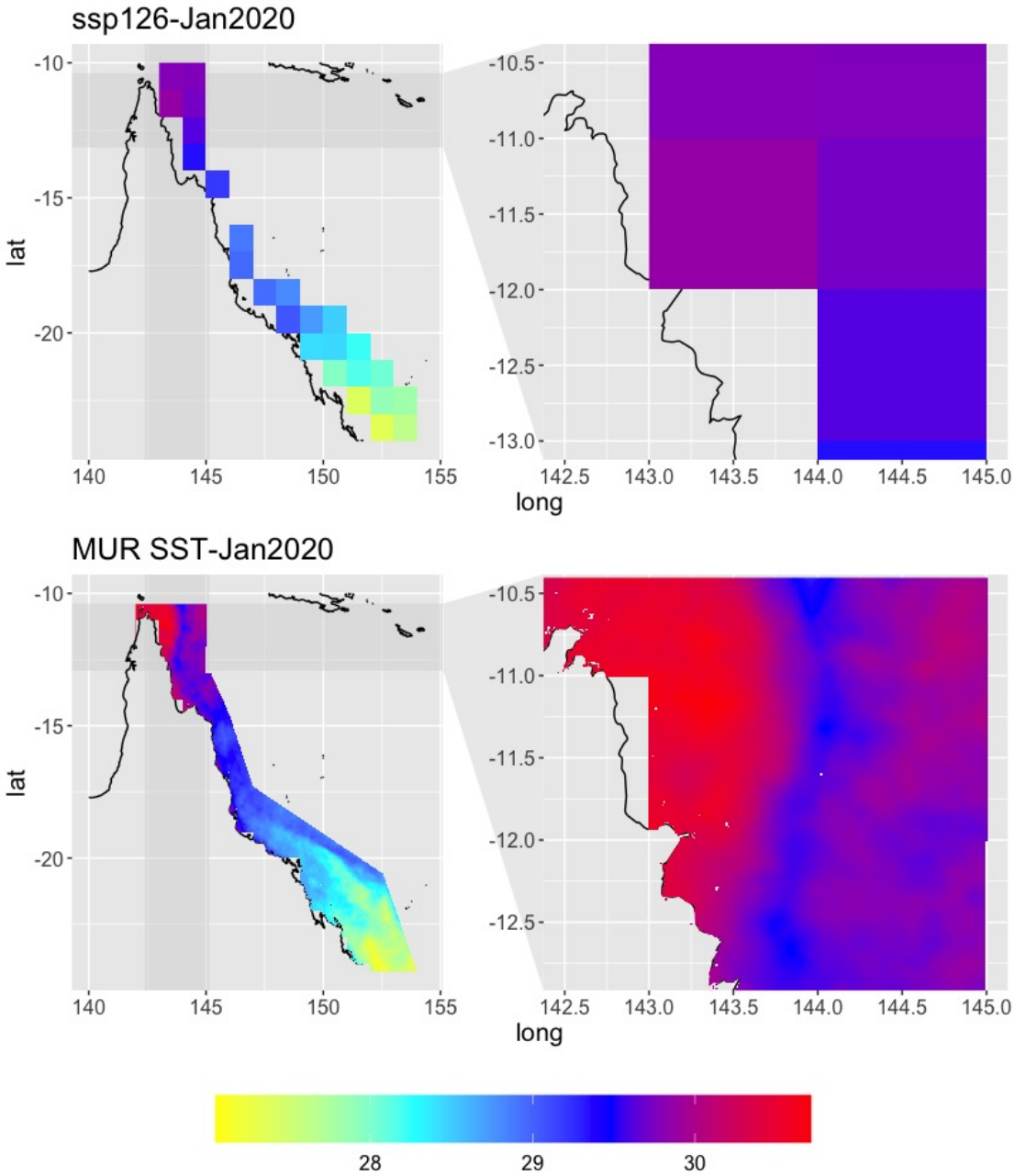
ssp126-Jan2020
-10
-15
-20
lat
140
145
150
155
-10.5
-11.0
-11.5
-12.0
-12.5
-13.0
142.5
143.0
143.5
144.0
144.5
145.0
long
MUR SST-Jan2020
-10
-15
-20
lat
140
145
150
155
-10.5
-11.0
-11.5
-12.0
-12.5
142.5
143.0
143.5
144.0
144.5
145.0
long
28
29
30

Related Work

- Van Hooidonk et al. (2015): Performed bias correction by adjusting the mean based on fine-resolution data and interpolated GCM outputs to a 4-km resolution grid.
  - Their method is a nonparametric regression using only spatial coordinates, without directly incorporating fine-resolution data.
- Ma et al. (2019): Developed a statistical downscaling method that generates fine-resolution outputs $\mathbf{Y}$ constrained such that the aggregated downscaled result matches the original coarse-resolution data, i.e., $\mathbf{AY} = \mathbf{X}$; demonstrated in simulation experiments.

Related Work (cont'd)

- Berrocal et al. (2010): Proposed a spatially varying coefficient model linking coarse-resolution model outputs (covariates) with fine-resolution in-situ observations (responses), applied for short-term projection downscaling using numerical model outputs and monitoring data.
- Harris et al. (2023): Integrated multi-model outputs using a neural network Gaussian Process (GP), treating GCM outputs as inputs and observations/reanalysis data as the output:

$$f_s : \mathbb{R}^{\sum_{i=1}^{m} q_i} \rightarrow \mathbb{R},$$

where $f_s(\cdot)$ is modeled as a GP and the input $\mathbf{x} \in \mathbb{R}^{\sum_{i=1}^{m} q_i}$ is an ensemble of m gridded GCM outputs, each with q_i grid points.

Initial Thoughts . . .

- We initially considered modeling $MUR_t(\mathbf{s})$ as the response, with $GCM_t(B)$ and spatial coordinates $\mathbf{s}$ as covariates:

$$f : \mathbb{R}^3 \to \mathbb{R}$$

  - Gaussian Processes (GPs) were considered due to their appealing properties:
    - Provide explicit predictive distributions and uncertainty quantification (UQ)
    - Supported by recent advances for scalable inference with large datasets
  - However, initial attempts were not successful:
    - GCM outputs differ substantially between the historical period (2002–2020, when MUR is available) and the projection period (2020–2099).
    - Using future GCM outputs directly as covariates can result in undesirable extrapolation behavior.
- We therefore chose to adopt a classical multivariate spatial modeling approach.

The Downscaling Framework

- We present a downscaling framework consisting of the following components:
  - **Preprocessing**: Apply bias correction and perform standard initial downscaling.
  - **Modeling**: Develop a bivariate spatial statistical model with two components:
    - **The mean structure, i.e., trend**
    - **Detrended residuals**
  - **Inference**: Fit the model and obtain downscaled fields from the predictive distributions.
- The resulting downscaled outputs demonstrate improved empirical predictive skill, computational efficiency, and support for uncertainty quantification.

Data Preprocessing

- Climate model outputs often exhibit systematic biases that must be corrected before further analysis.
- We adopt the bias correction and interpolation method of Van Hooidonk et al. (2015), applying the following steps to each monthly snapshot:

1. Subtract the multi-year mean GCM SST (2002–2020) at coarse resolution
   ↓
2. Interpolate the residual to fine resolution using spline interpolation
   ↓
3. Add the multi-year mean MUR SST (2002–2020) at fine resolution

- The resulting bias-corrected, fine-resolution fields are denoted by $GCM_{m,y}(\mathbf{s})$, where m is the month, y is the year, and $\mathbf{s}$ denotes the spatial grid location.

Modeling Framework

- We adopt an additive modeling framework commonly used in spatial statistics:

$$\text{Spatio-temporal Dynamics} + \text{Seasonal Large-scale Spatial Variability}$$

$$+ \text{Small-scale Spatial Variability (Independent Over Time)}$$

- The first two components together define the trend.
- The final component, representing detrended residuals, will be modeled using a bivariate spatial model.
- We adopt a two-stage modeling strategy:
  - **Stage 1**: Estimate the trend.
  - **Stage 2**: Model the time-independent detrended residuals.

Modeling the Trend

- The trend is modeled as the sum of two components:

  Spatio-temporal Dynamics + Seasonal Large-Scale Spatial Variability

  - Spatio-temporal Dynamics: A nonstationary component that varies across space and time, with dynamics that change by month.
  - Seasonal Large-Scale Spatial Variability: A spatial component that captures large-scale spatial pattern for a given season.

- The common spatio-temporal dynamics term, denoted $\mu_{m,y}(s)$, is included in the trend for both $MUR_{m,y}(s)$ and $GCM_{m,y}(s)$.
- We estimate $\mu_{m,y}(s)$ using a 5-year moving average of GCM outputs for month m and location s:

$$\hat{\mu}_{m,y}(s) = \frac{1}{5}\sum_{i=1}^{5} GCM_{m,y-i}(s).$$

- The extended time span of GCM data (pre-2002 to 2099) enables the use of moving averages even beyond the time period with MUR data.

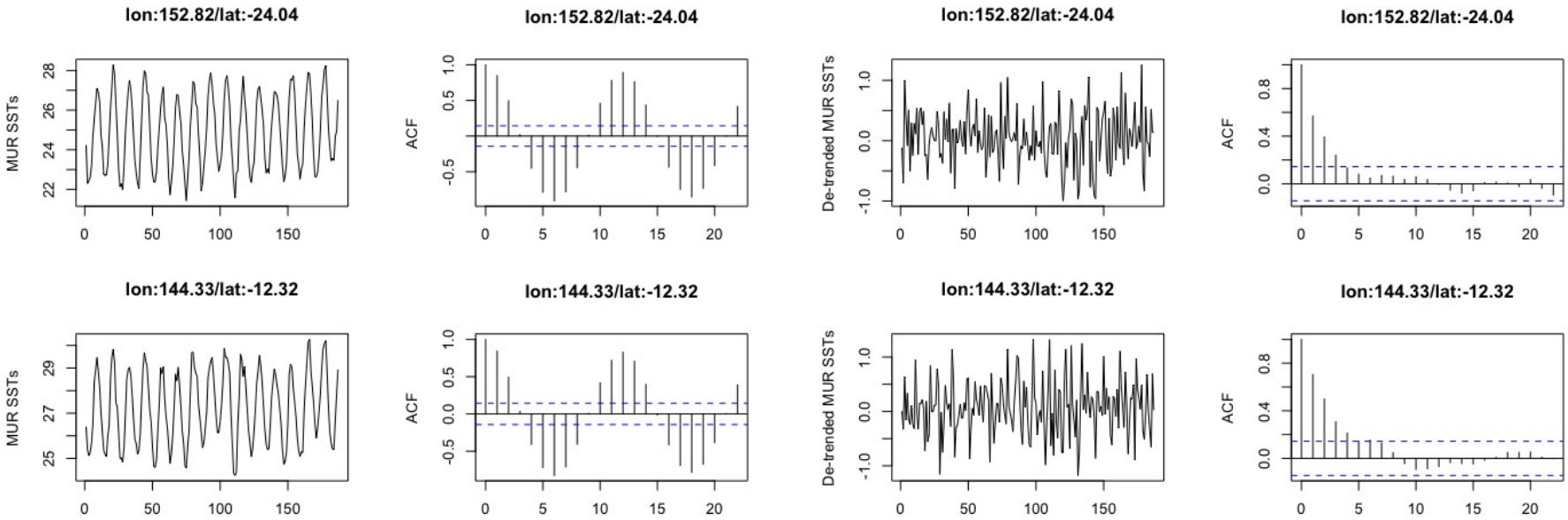

Left panels display the time series and autocorrelation function (ACF) plots from the MUR SST data at two randomly selected fine-resolution pixels, revealing strong seasonality and temporal dependence. In contrast, the right panels show the same plots after subtracting the estimated $\hat{\mu}_{m,y}(s)$ from the MUR SST data, demonstrating a significant reduction in temporal dependence.

Seasonal Large-Scale Spatial Variability

- To simplify notation, we denote the MUR SST data and preprocessed GCM outputs, each adjusted by subtracting the estimated $\hat{\mu}_{m,y}(s_i)$, as

$$Y_{t,1}(s_i) \quad \text{and} \quad Y_{t,2}(s_i), \quad i = 1, \ldots, N; \quad t = 1, \ldots, T_o,$$

  omitting explicit year and season subscripts for clarity.
  - Here, T_o is the number of months in the observational period for the given season. For example, for summer (December–February)[1]:

$$T_o = 3 \times (2020 - 2002) + 1 = 55.$$

  - The study domain consists of $N = 309{,}700$ fine-resolution pixels.

[1] MUR data are from June 2002 to December 2020.

EOFs for Each Season

- For each season, we have bivariate datasets

$$\{(Y_{t,1}(s_i), Y_{t,2}(s_i))' : i = 1, \ldots, N; t = 1, \ldots, T_o\}$$

  corresponding to MUR ($i = 1$) and GCM ($i = 2$).
- We apply Singular Value Decomposition (SVD) to the resulting $N \times (2T_o)$ matrix to extract Empirical Orthogonal Functions (EOFs).
  - EOFs are calculated using only months where both MUR and GCM data are available, ensuring balanced representation and leveraging the strength of MUR data in downscaling.
- A subset of K EOFs, denoted $U^k(s)$, are used to described the seasonal spatial variablity tructure.mean structure:

$$\sum_{k=1}^{K} U^k(s)\xi_i^k,$$

  where $i = 1$ for MUR and $i = 2$ for GCM.

Remarks on the Trend

- The trend component captures nonstationary spatio-temporal structure using:
  - 5-year moving averages of GCM data (within each month) to estimate shared temporal dynamics.
  - Empirical Orthogonal Functions (EOFs) computed seasonally, used as fixed-effect spatial covariates.
- While the same EOFs are applied to both MUR and GCM data, separate coefficient vectors $\boldsymbol{\xi}_1$ and $\boldsymbol{\xi}_2$ are estimated for each.
- Monthly EOFs were considered but resulted in too few basis functions and degraded downscaling performance.

Modeling the Detrended Residuals

- After removing the estimated trend, we define the residual process as:

$$Z_{t,i}(s) = Y_{t,i}(s) - \hat{\mu}_{t,i}(s), \quad \text{where} \quad \hat{\mu}_{t,i}(s) = \sum_{k=1}^{K} U^k(s)\hat{\xi}_i^k,$$

where

- $i = 1$: residuals from MUR data
- $i = 2$: residuals from GCM outputs

- The residuals are modeled using a spatial model based on basis functions (Nguyen et al., 2012; Krock et al., 2020):

$$Z_{t,i}(s) = \sum_{l=1}^{L} S^l(s)\eta_{t,i}^l + \epsilon_{t,i}(s), \quad i = 1, 2,$$

where:

  - $S^l(s)$: Prespecified spatial basis functions;
  - $\eta_{t,i}^l$: Random coefficients that vary across time and data source;
  - $\epsilon_{t,i}(s) \sim \mathrm{N}(0, \tau_i^2)$: Gaussian white noise process, independent of the random effects $\eta_{t,i}^l$.

- For a given time point t, define the bivariate residual vector at location s_n as:

$$\mathbf{Z}_t(s_n) = \begin{pmatrix} Z_{t,1}(s_n) \\ Z_{t,2}(s_n) \end{pmatrix}, \quad n = 1, \ldots, N.$$

- The full spatial model across all N pixels can be written as:

$$\begin{pmatrix} \mathbf{Z}_t(s_1) \\ \vdots \\ \mathbf{Z}_t(s_N) \end{pmatrix} = \begin{pmatrix} \mathbf{S}(s_1) \otimes \mathbf{I}_2 \\ \vdots \\ \mathbf{S}(s_N) \otimes \mathbf{I}_2 \end{pmatrix} \begin{pmatrix} \boldsymbol{\eta}_t^1 \\ \vdots \\ \boldsymbol{\eta}_t^L \end{pmatrix} + \begin{pmatrix} \boldsymbol{\varepsilon}_t(s_1) \\ \vdots \\ \boldsymbol{\varepsilon}_t(s_N) \end{pmatrix},$$

  - $\mathbf{S}(s_n) = \big(S^1(s_n), \ldots, S^L(s_n)\big)$: vector of spatial basis functions at $\mathbf{s}_n$;
  - $\boldsymbol{\eta}_t^l = \begin{pmatrix} \eta_{t,1}^l \\ \eta_{t,2}^l \end{pmatrix}$: random effect vector associated with the lth basis function $S^l(\cdot)$;
  - $\boldsymbol{\varepsilon}_t(s_n) = \begin{pmatrix} \epsilon_{t,1}(s_n) \\ \epsilon_{t,2}(s_n) \end{pmatrix}$: bivariate Gaussian white noise process;
  - $\boldsymbol{\eta}_t^l \sim \mathcal{N}(0, \mathbf{Q}_l^{-1})$, independently over time.

- The model can be further expressed in compact form as:

$$\underset{2N\times 1}{\mathbf{Z}_t} = \underset{2N\times 2L}{\mathbb{S}}\ \underset{2L\times 1}{\boldsymbol{\eta}_t} + \underset{2N\times 1}{\boldsymbol{\varepsilon}_t},$$

where:

- $\mathbf{Z}_t = (\mathbf{Z}_t(s_1)', \ldots, \mathbf{Z}_t(s_N)')'$: full bivariate residual vector,
- $\mathbb{S} = \mathbf{S} \otimes \mathbf{I}_2$, with $\mathbf{S} = \big(\mathbf{S}(s_1), \ldots, \mathbf{S}(s_N)\big)' \in \mathbb{R}^{N\times L}$,
- $\boldsymbol{\eta}_t = (\boldsymbol{\eta}_t^{1'}, \ldots, \boldsymbol{\eta}_t^{L'})' \in \mathbb{R}^{2L}$: stacked random effect vector,
- $\boldsymbol{\varepsilon}_t = (\boldsymbol{\varepsilon}_t(s_1)', \ldots, \boldsymbol{\varepsilon}_t(s_N)')'$: bivariate noise vector.

Remarks on the Model

$$\underset{2N\times 1}{\mathbf{Z}_t} = \underset{2N\times 2L}{\mathcal{S}}\ \underset{2L\times 1}{\boldsymbol{\eta}_t} + \underset{2N\times 1}{\boldsymbol{\varepsilon}_t},$$

- It defines a **low-rank spatial model** with $L \ll N$:
  - Describes nonstationary spatial dependence via EOF basis functions,
  - Reduces computational cost through low-rank matrices.
- The random effect vectors $\boldsymbol{\eta}_t^l$ are **independent across basis levels** $l = 1, \ldots, L$, following the multivariate Basis Graphical Lasso (BGL) framework (Krock et al., 2023).
- This leads to a block-diagonal precision matrix for $\boldsymbol{\eta}_t$:

$$\mathbf{Q} = \text{blockdiag}(\mathbf{Q}_1, \ldots, \mathbf{Q}_L),$$

where each block $\mathbf{Q}_l$ describe the conditional dependence between MUR and GCM components associated with the lth basis function.

Estimation Procedure

- We adopt a two-stage estimation approach:
  - **Stage 1:** Estimate the trend.
  - **Stage 2:** Estimate remaining parameters by minimizing:

$$\text{Negative Log-Likelihood} + \ell_1\text{-Fusion Penalty},$$

where the penalty is defined as:

$$P(\mathbf{Q}) = \rho \sum_{l=1}^{L-1} \sum_{i \neq j} \left| (\mathbf{Q}_l)_{ij} - (\mathbf{Q}_{l+1})_{ij} \right|.$$

This fusion penalty encourages similarity between the off-diagonal elements of adjacent precision matrices $\mathbf{Q}_l$ and $\mathbf{Q}_{l+1}$, associated with consecutive basis functions.

Negative Log-Likelihood of the Model

We consider the negative log-likelihood (up to a constant), given by:

$$\log\det(\mathcal{S}\mathbf{Q}^{-1}\mathcal{S}' + \mathbf{D}) + \operatorname{tr}\left(\hat{\mathbf{\Sigma}}(\mathcal{S}\mathbf{Q}^{-1}\mathcal{S}' + \mathbf{D})^{-1}\right), \tag{1}$$

where:

- $\hat{\mathbf{\Sigma}} = \frac{1}{T_o}\sum_{t=1}^{T_o}\mathbf{Z}_t\mathbf{Z}_t'$ is the sample covariance matrix,
- T_o is the total number of time points,
- $\mathbf{D} = \mathbf{I}_N \otimes \operatorname{diag}(\tau_1^2, \tau_2^2)$, with $\mathbf{I}_N$ as the $N \times N$ identity matrix.

Penalized Likelihood Estimation

The objective function for parameter estimation is based on penalized maximum likelihood with an ℓ_1-fusion penalty:

$$\hat{\mathbf{Q}} \in \underset{\mathbf{Q} \succeq 0}{\arg\min} \log\det(\mathcal{S}\mathbf{Q}^{-1}\mathcal{S}' + \mathbf{D}) + \operatorname{tr}\left(\hat{\mathbf{\Sigma}}(\mathcal{S}\mathbf{Q}^{-1}\mathcal{S}' + \mathbf{D})^{-1}\right) + P(\mathbf{Q})$$

where the fusion penalty is defined as:

$$P(\mathbf{Q}) = \rho \sum_{l=1}^{L-1} \sum_{i \neq j} |(\mathbf{Q}_l)_{ij} - (\mathbf{Q}_{l+1})_{ij}| \,.$$

- To reduce computational complexity, we apply the Sherman–Morrison–Woodbury formula to reformulate the likelihood.
- The expression remains non-convex in $\mathbf{Q}$. A difference-of-convex (DC) algorithm for estimation (Krock et al., 2023) is used. At each iteration, the concave part is linearized around the current estimate, and a convex optimization problem is solved.

Downscaling

- Recall the spatial model:

$$Z_{t,i}(s) = \sum_{l=1}^{L} S^l(s)\,\eta_{t,i}^l + \epsilon_{t,i}(s), \quad i = 1, 2,$$

- When only GCM data $\mathbf{Z}_{t,2} = \left(Z_{t,2}(\mathbf{s}_1), \ldots, Z_{t,2}(\mathbf{s}_N)\right)'$ is available, the downscaling task is to obtain the conditional distribution $\mathbf{Z}_{t,1} \mid \mathbf{Z}_{t,2}$ (with the mean structure added back).
- Based on the basis function representation, this requires evaluating the conditional distribution:

$$\boldsymbol{\eta}_{t,1} \mid \mathbf{Z}_{t,2},$$

which is multivariate normal. Its mean and variance can be derived using standard results for the conditional distribution of a multivariate normal vector (formulas omitted).

Validation Studies

- We conducte two validation studies:
  - **Validation with MUR:**
    - Methods were implemented using GCM outputs and MUR data from June 2002 to December 2017.
    - The downscaled SSTs were then evaluated against held-out MUR data from 2018 to 2020.
  - **Validation with Synthetic Data:**
    - We interpolate outputs from another GCM, treating these as "synthetic" MUR data.
    - Using GCM outputs and synthetic MUR data from June 2002 to December 2017, we fit the model.
    - Downscaled SSTs were generated and compared with the synthetic MUR data for the extended period from January 2018 to December 2099.

- We compare our method, denoted by **BGL**, with the following approaches:
  1. **GCM:** Direct interpolation of GCM outputs to the fine-resolution grid.
  2. **Std:** The standard downscaling method from Van Hooidonk et al. (2015). *[bias correction + interpolation]*
  3. **laGP:** The local approximate Gaussian Process method (Gramacy and Apley, 2015), used to model detrended MUR residuals. Inputs include detrended GCM residuals and spatial coordinates (longitude and latitude), $f : \mathbb{R}^3 \to \mathbb{R}$. *[laGP is computationally efficient and able to describe nonstationary dependence.]*
  4. **MFRK:** The multivariate Fixed Rank Kriging model (Nguyen et al., 2012). *[Same basis functions but without assuming independence across basis function levels and without the L1 penalty]*

Quantitative Metrics for Predictive Performance

- **Mean Squared Error (MSE):** Computed across the spatial domain and/or a validation time period.
- **Continuous Ranked Probability Score (CRPS):** Measures accuracy of the predictive distribution; lower scores indicate better performance (Gneiting et al., 2005).
- **Empirical Coverage:** Proportion of held out SST values contained within predictive confidence intervals across fine-resolution pixels.
- **Interval Score:** Penalizes both wide intervals and deviations from observed values; lower scores indicate more accurate and precise predictive intervals (Gneiting and Raftery, 2007).

Validation with MUR Data

Table: MSE values calculated across locations, averaged over months, and grouped by seasons from MUR validation under SSP585.

Season	GCM	Std	laGP	MFRK	BGL
Summer	0.399	0.288	0.443	0.375	0.304
Autumn	0.489	0.112	0.225	0.186	0.089
Winter	0.886	0.260	0.347	0.288	0.203
Spring	0.430	0.254	0.399	0.235	0.167
Overall	0.551	0.228	0.353	0.261	0.185

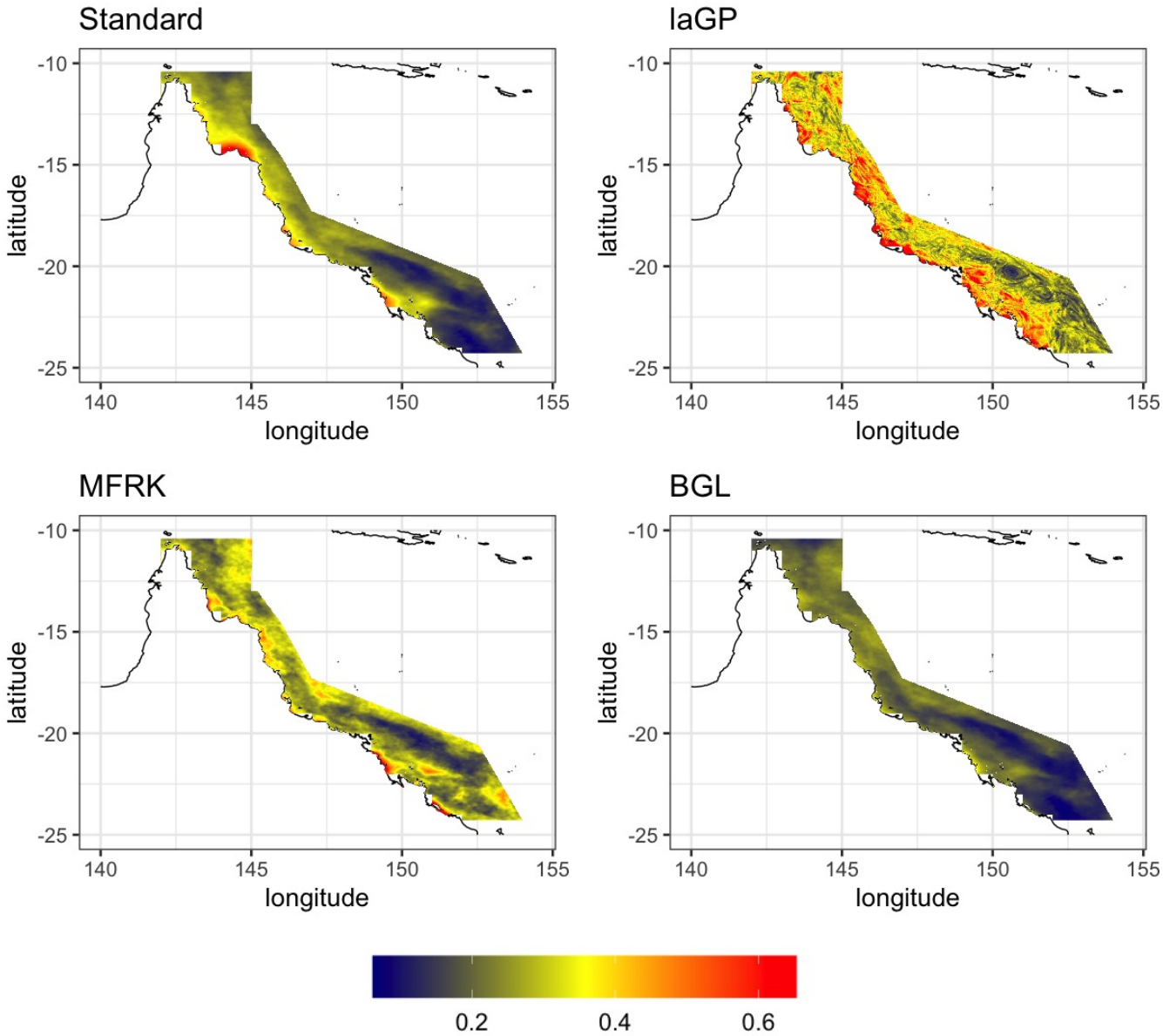

Maps of MSE from MUR validation under SSP585.

Table: CRPS, interval scores, and empirical coverages from MUR validation under SSP585.

CRPS			
Season	laGP	MFRK	BGL
Summer	0.451	0.350	0.314
Autumn	0.304	0.244	0.182
Winter	0.382	0.303	0.263
Spring	0.404	0.272	0.235
Interval score			
Season	laGP	MFRK	BGL
Summer	0.312	0.129	0.112
Autumn	0.191	0.101	0.097
Winter	0.240	0.113	0.128
Spring	0.258	0.114	0.107
Coverage			
Season	laGP	MFRK	BGL
Summer	33.04%	69.91%	73.57%
Autumn	42.21%	78.67%	80.99%
Winter	40.64%	76.12%	80.46%
Spring	41.16%	78.41%	80.43%

Validation with Synthetic Data

- Results are consistent with validation using MUR data:
  - BGL achieves the lowest MSE.
  - BGL also shows better performance in terms of CRPS, interval score, and empirical coverage.

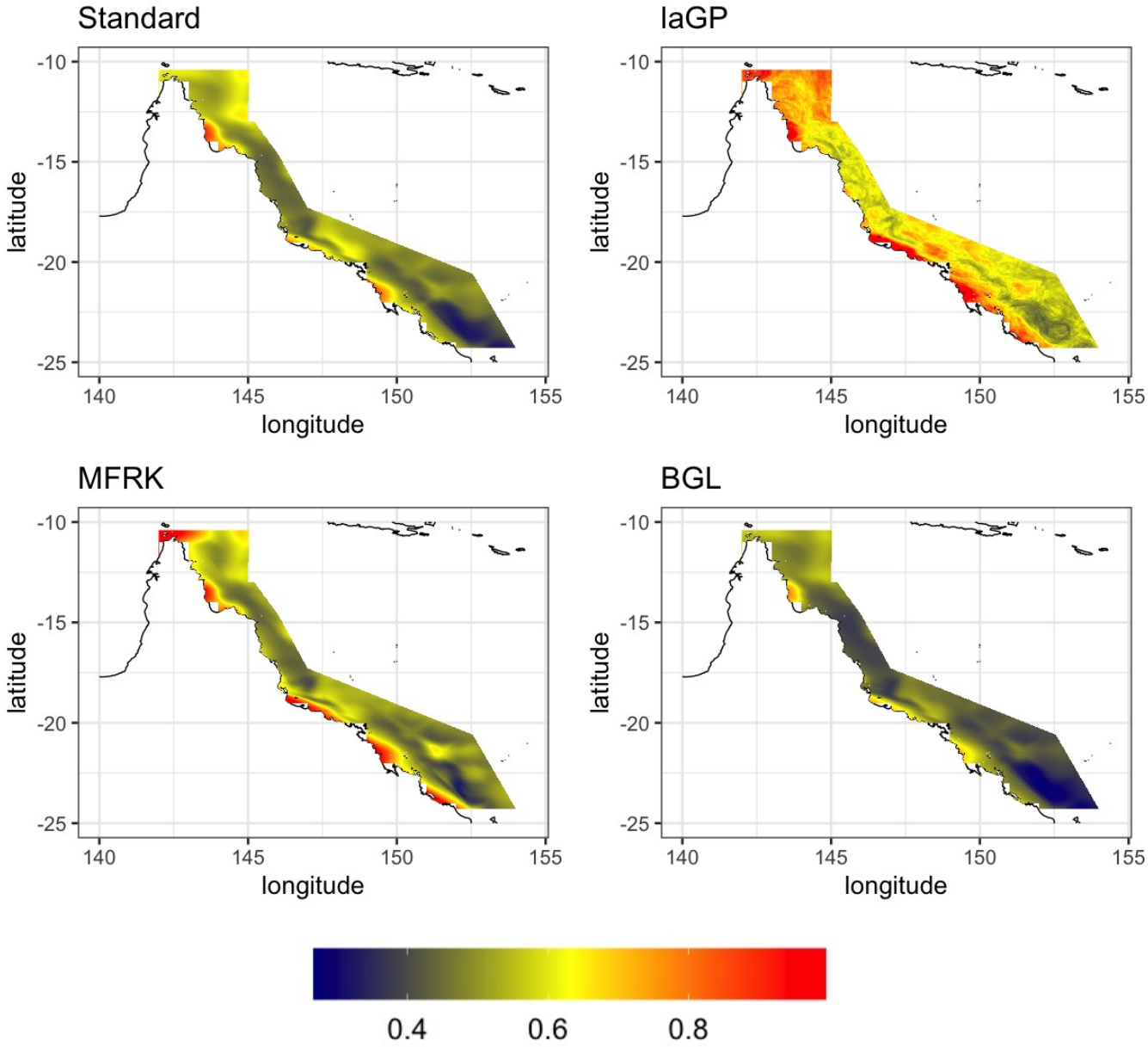

Maps of MSE from synthetic validation under SSP585.

Additional Results: SSP126 vs. SSP585

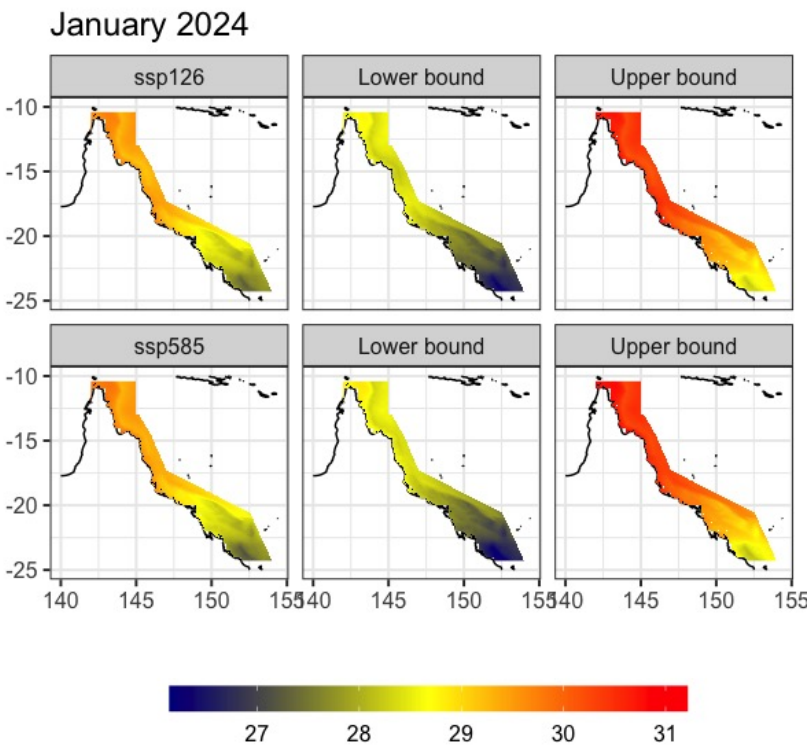

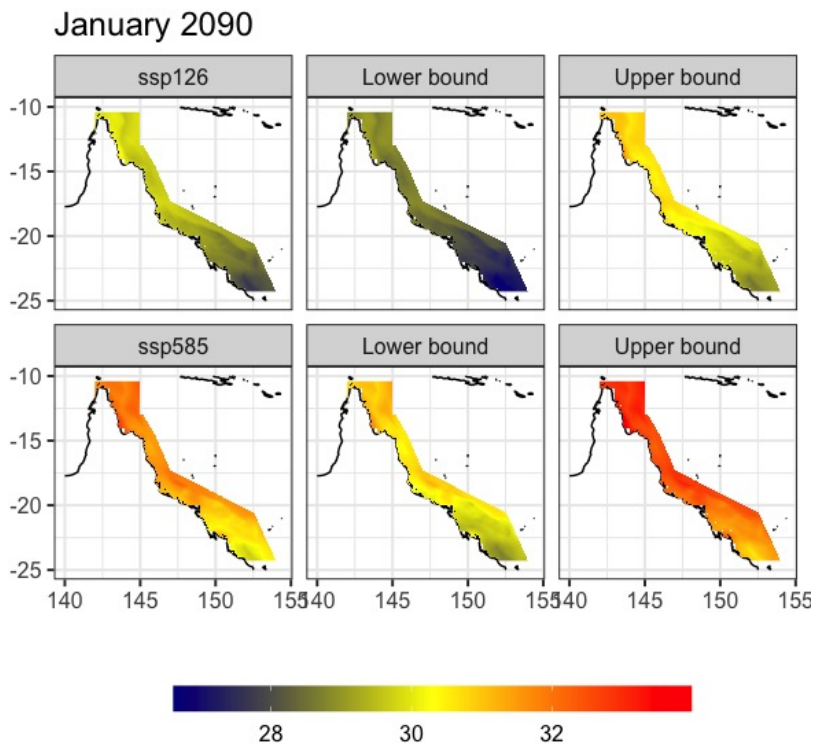

Projected SST Changes Over Coastal Regions

- Lima and Wethey (2012) reported that 72% of coastal regions experienced significant SST increases, with an average warming rate of 0.25°C per decade (1982–2010).
- To assess future changes, we use downscaled SST projections to evaluate decadal shifts relative to recent averages.
  - Specifically, we calculate the decadal mean January SST at each pixel using MUR data from 2010 to 2020.
  - For future years $T^* = 2020 + 10i$ with $i = 1, 2, \ldots, 7$, we compute the pointwise probability that January SST exceeds the 2010–2020 mean by a threshold of $0.25i$°C, leveraging the predictive distribution.
  - For example:
    - Probability that January 2030 SST $>$ 2010–2020 mean + 0.25°C
    - Probability that January 2040 SST $>$ 2010–2020 mean + 0.5°C
    - And so forth...

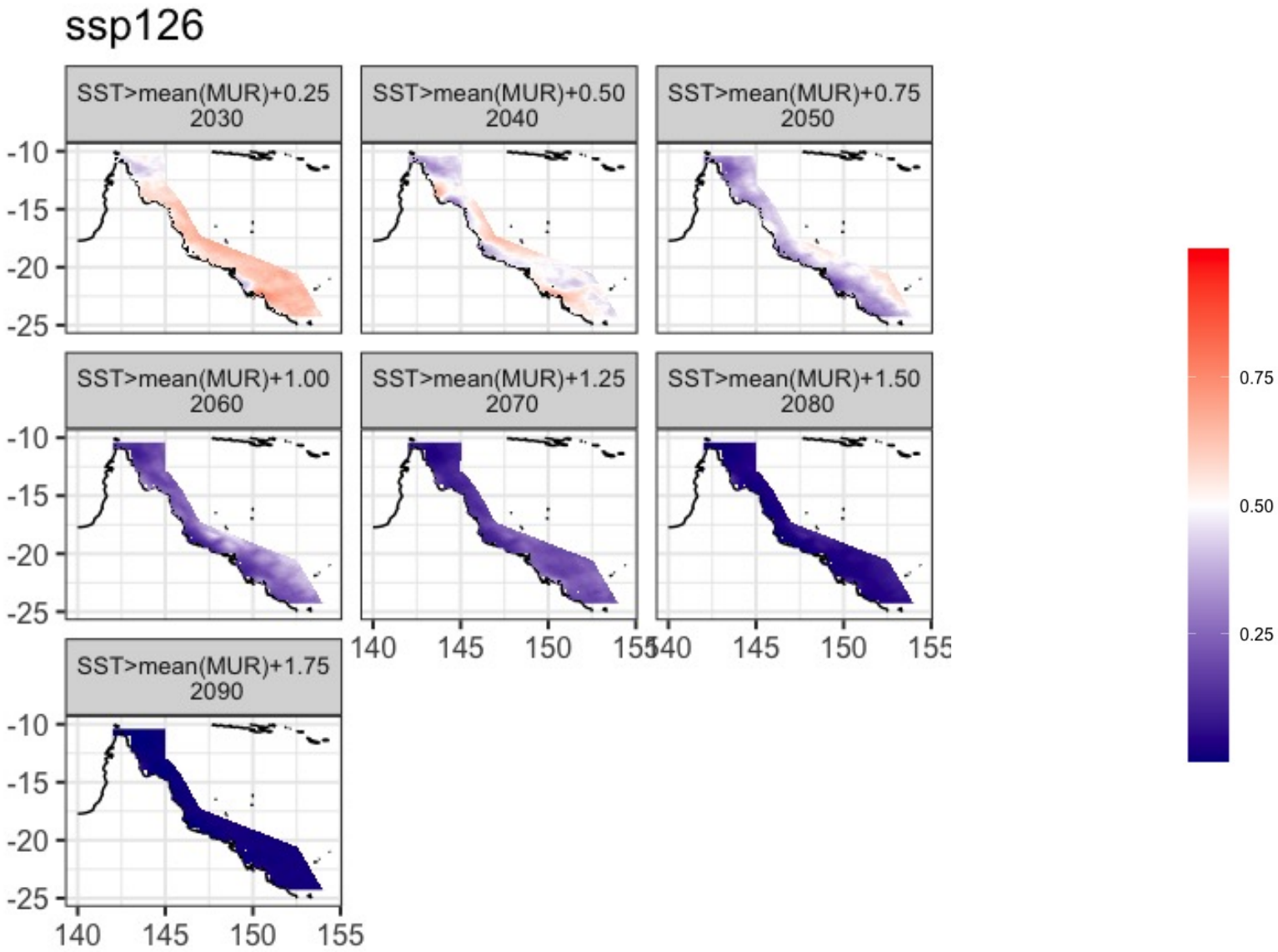
ssp126
SST>mean(MUR)+0.25
2030
SST>mean(MUR)+0.50
2040
SST>mean(MUR)+0.75
2050
SST>mean(MUR)+1.00
2060
SST>mean(MUR)+1.25
2070
SST>mean(MUR)+1.50
2080
SST>mean(MUR)+1.75
2090
-10
-15
-20
-25
140
145
150
155
0.75
0.50
0.25

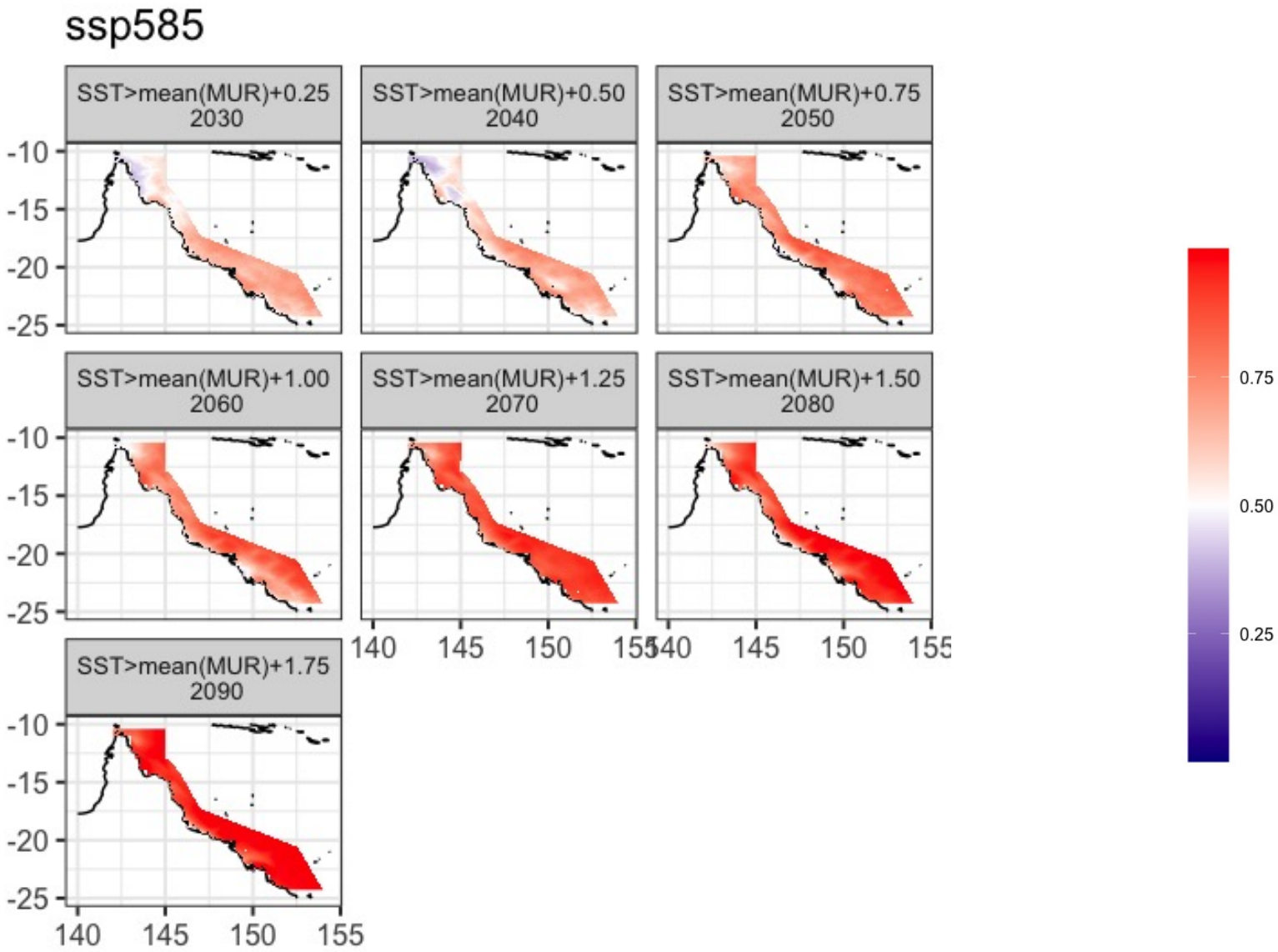
ssp585
SST>mean(MUR)+0.25
2030
SST>mean(MUR)+0.50
2040
SST>mean(MUR)+0.75
2050
SST>mean(MUR)+1.00
2060
SST>mean(MUR)+1.25
2070
SST>mean(MUR)+1.50
2080
SST>mean(MUR)+1.75
2090
-10
-15
-20
-25
140
145
150
155
0.75
0.50
0.25

Discussion

- Empirical downscaling results are good, but it is important to recognize inherent limitations such as uncertainty in parameter estimation and model assumptions.
- How can we integrate outputs from multiple GCMs to produce a unified downscaling product?
  - The Basis Graphical Lasso (BGL) offers a scalable solution for handling highly multivariate settings involving $(K+1) \times (K+1)$ precision matrices $\mathbf{Q}^{I}$, where K denotes the number of GCMs.
  - Harris et al. (2023) propose Gaussian processes with covariance functions derived from infinitely wide deep neural networks.
  - Bayesian model averaging and Bayesian model mixing (Yannotty et al., 2024) provide promising approaches for combining multiple models within a coherent probabilistic framework.

Discussion: Joint Modeling vs. Conditional Modeling

- Instead of jointly modeling GCM and MUR data, we can model their distribution conditionally, as done in multi-fidelity computer experiments:
  - $GCM(s,t)$ — analogous to the low-fidelity model output.
  - $MUR(s,t) \mid GCM(s,t)$ — the high-fidelity output conditional on the low-fidelity output.
  - Combining physics and data:
    - One extension is to generalize the current model to an autoregressive co-kriging framework for multi-fidelity outputs, treating observations, regional climate model outputs, and global climate model outputs as high-, medium-, and low-fidelity data respectively.

Additional Thoughts and Lessons Learned

- Striking a balance between general modeling frameworks and careful implementation:
  - Gaussian Processes (GPs): Direct use of GCM outputs as inputs may cause problematic extrapolation.
  - An additive model structure: separating trend and residual components.
- Be prepared to make modeling choices and understand their implications:
  - Assumptions such as independence and stationarity.
  - Decisions about nodes, layers, and the number of basis functions.
- Maintain an open mind!

Coral Watch

- Source: https://coralwatch.org/

Acknowledgements

- This work is partially funded by, NASA/JPL, NSF (DMS-2053668), Simons Foundation's Collaboration Award (#317298 and #712755), University Research Council (URC), and TAFT research center at University of Cincinnati.

Thank you!